

A common solution to R_D anomalies and Dark Matter

G. Bélanger¹, J. Bernigaud^{2,3,4}, A. Bharucha⁵, B. Fuks⁶, J. Heisig⁷, A. Jueid¹, A. Goudelis⁶, A. Lessa⁸, D. Marzocca⁹, M. Nardecchia¹⁰, G. Polesello¹¹, P. Pani¹², D. Sengupta¹⁴ and J. Zurita^{3,4}.

¹LAPTh, Univ. Grenoble Alpes, USMB, CNRS, LAPTh, 74940 Annecy, France,

² Univ. Grenoble Alpes, Univ. Savoie Mont Blanc, CNRS, LAPTh, 9 Chemin de Bellevue, F-74000 Annecy, France,

³ Institute for Nuclear Physics (IKP), KIT Karlsruhe Institute of Technology, Hermann-von-Helmholtz-Platz 1, D-76344 Eggenstein-Leopoldshafen, Germany

⁴Institute for Theoretical Particle Physics (TTP), Karlsruhe Institute of Technology, EngesserstraÙ e 7, D-76128 Karlsruhe, Germany

⁵ Laboratoire d'Annecy-le-Vieux de Physique Theorique LAPTh, CNRS ? USMB, BP 110 Annecy-le-Vieux, F-74941 Annecy, France,

⁶ LPTHE, UMR 7589 - CNRS and Sorbonne Université, 75252 Paris Cedex, France and Sorbonne Universités, Institut Lagrange de Paris (ILP), 98 bis Boulevard Arago, 75014 Paris, France,

⁷ Centre for Cosmology, Particle Physics and Phenomenology (CP3), Université catholique de Louvain, Chemin du Cyclotron 2, B-1348 Louvain-la-Neuve, Belgium

⁸ Centro de Ciências Naturais e Humanas, Universidade Federal do ABC, Santo André, 09210-580 SP, Brazil,

⁹ INFN Sezione di Trieste, via Bonomea 265, 34136 Trieste, Italy

¹⁰ Sapienza - Università di Roma, Piazzale Aldo Moro 2, 00185, Roma, Italy,

¹¹ INFN, Sezione di Pavia, Via Bassi 6, 27100 Pavia, Italy,

¹² Deutsches Elektronen Synchrotron, DESY, 15738 Zeuthen, Germany

¹³ Department of Physics and Astronomy, 9500 Gilman Drive, University of California, San Diego.

Abstract

The anomalies observed by LHCb in flavor observables suggest the breakdown of lepton flavor universality. We study how a vanilla leptoquark solution to the $R_{D^{(*)}}$ anomalies can also explain the measured relic abundance, if the leptoquark mediates between the visible sector and the dark sector. We find that [something awesome].

1. INTRODUCTION

The current LHC dataset has not shown any significant deviation from the SM expectations, except for the $R_{K^{(*)}}$ [1, 2] and $R_{D^{(*)}}$ [3, 4, 5] anomalies. While many models have been considered to explain these observations, the consensus is that two classes of models can accommodate these results: leptoquarks and Z' models (for a recent review see e.g [6] and references therein). It is thus interesting to consider the interplay between these solutions and dark matter (DM), which essentially requires to add an additional decay of the leptoquark into the dark sector, studied previously in [7, 8]. As this will reduce the visible decays of the leptoquarks, this naively allows to lower the current expectation of $m_{LQ} \gtrsim 1$ TeV with $\mathcal{O}(1)$ couplings, thus opening up novel parameter space and increasing the opportunities to probe this model at the LHC in the near future.

For our study we built a simplified model featuring the minimal ingredients to explain the charged current flavor anomalies $R_{D^{(*)}}$ and dark matter simultaneously, limiting ourselves to the couplings strictly

necessary to explain the anomaly. We study how the different phenomenological constraints affect the parameter space: LHC searches for leptoquarks and dark matter, relic density and direct detection. We pay particular attention to the existing CMS search for a resonant leptoquark plus missing energy: while this search might not always be the golden channel for discovery, its importance lies in the fact that this is indeed probing the $R_{D^{(*)}}$ -DM connection (RDM).

2. THE MODEL

[JZ: Text taken from Benj, except for last paragraph.]

We consider a simplified model in which we supplement the Standard Model by one scalar leptoquark field S_1 and two extra fermionic fields, a Majorana fermion χ_0 and a Dirac fermion χ_1 . The S_1 and χ_1 fields are electrically-charged coloured weak singlets lying in the $(\mathbf{3}, \mathbf{1})_{-1/3}$ representation of the Standard Model gauge group. In contrast, χ_0 is a dark matter candidate and therefore a non-coloured electroweak singlet. In our FEYNRULES implementation, we consider all potential interactions of the new sector with the Standard Model sector, the corresponding Lagrangian being written as

$$\mathcal{L} = \mathcal{L}_{\text{SM}} + \mathcal{L}_{\text{kin}} + \left[\lambda_R \bar{u}_R^c \ell_R S_1^\dagger + \lambda_L \bar{Q}_L^c \cdot L_L S_1^\dagger + y_\chi \bar{\chi}_1 \chi_0 S_1 + \text{h.c.} \right]. \quad (1)$$

In this expression, all flavour indices are understood for simplicity and the dot stands for the $SU(2)$ -invariant product of two fields lying in its fundamental representation. In addition, \mathcal{L}_{SM} is the Standard Model Lagrangian and \mathcal{L}_{kin} contains gauge-invariant kinetic and mass terms for all new fields, the χ_1 state being assumed vector-like. The Q_L and L_L spinors stand for the $SU(2)_L$ doublets of left-handed quarks and leptons respectively, whilst u_R and ℓ_R stand for the $SU(2)_L$ singlets of right-handed down-type quarks and charged leptons, respectively. As can be derived from the omitted flavour structure, the λ_L and λ_R couplings are 3×3 matrices in the flavour space, that are considered real in the following. Moreover, in our conventions, the first index i of any λ_{ij} element refers to the quark generation whilst the second one j refers to the lepton generation.

The field content of the new physics sector of our simplified model is presented in table 1, together with the corresponding representation under the gauge and Poincaré groups, the potential Majorana nature of the different particles, the adopted symbol in the FEYNRULES implementation and the PDG identifier that has been chosen for each particle. The new physics coupling parameters are collected in table 2, in which we additionally include the name used in the FEYNRULES model and the Les Houches blocks in which the numerical values of the different parameters can be changed by the user when running tools like MG5_AMC or MICROMEGAS.

Field	Spin	Repr.	Self-conj.	FEYNRULES name	PDG code
S_1	0	$(\mathbf{3}, \mathbf{1})_{-1/3}$	no	LQ	42
χ_0	1/2	$(\mathbf{1}, \mathbf{1})_0$	yes	chi0	5000521
χ_1	1/2	$(\mathbf{3}, \mathbf{1})_{-1/3}$	no	chi1	5000522

Table 1: New particles supplementing the Standard Model, given together with the representations under $SU(3)_c \times SU(2)_L \times U(1)_Y$. We additionally indicate whether the particles are Majorana particles, their name in the FEYNRULES implementation and the associated Particle Data Group (PDG) identifier.

Coupling	FEYNRULES name	Les Houches block
$(\lambda_L)_{ij}$	lamL	LQLAML
$(\lambda_R)_{ij}$	lamR	LQLAMR
y_χ	yDM	DMINPUTS

Table 2: *Couplings of the new particles, given together with the associated FEYNRULES symbol and the Les Houches block of the parameter card.*

In a nutshell, our model needs three new masses and several new couplings. The R_D anomalies can be solved with only $(\lambda_L)_{33} \equiv \lambda_L$ ¹ and $(\lambda_R)_{23} \equiv \lambda_R$. Finally, the dark matter phenomenology requires the coupling y_χ . Hence these 6 parameters span our parameter space. In what follows we will study how the flavor anomalies, dark matter phenomenology and collider searches constrain this parameter space, showing the currently allowed parameter space and commenting on the future prospects.

3. LEPTOQUARK SOLUTIONS TO R_D ANOMALIES

As mentioned in the previous chapter, a minimal solution of the $R(D)$ anomalies can be obtained with just a left-handed (33) and a right-handed (32) couplings to S_1 . We note that the 33 coupling is forced to be left-handed due to the presence of the neutrino². The choice of having a right-handed coupling for the 32 interaction is due to the large contributions that a left-handed coupling would generate to the $B \rightarrow X_s \nu \nu$ process, which in turn would require the addition of another leptoquark state [10, 11, 12, 13]. We perform a global fit of the model with the two couplings $(\lambda_L)_{33}$ and $(\lambda_R)_{23}$ as free parameters. The relevant observables included in the fit are: R_D , R_D^* , $\text{Br}(B_c \rightarrow \tau \nu)$, deviations in the Z couplings to τ_L and τ_R , effective number of neutrinos from Z decays, lepton flavour universality test in τ decays. For more details on this fit see e.g. [11, 12, 9]. A contribution to $D^0 - \bar{D}^0$ mixing is generated at one loop, but it is strongly CKM-suppressed and does not provide a strong constraint. The results of a scan in the two parameters of the model, for $m_{S_1} = 1.5 \text{ TeV}$, where all points are within 1σ of the best-fit point, is shown in the plane of the R_D and R_D^* anomalies in the left panel of figure 1. The corresponding preferred region in the two couplings is presented in the right panel of figure 1.³

From the figure we can establish two working points. We pick the first one to obtain the lowest possible $BR(S_1 \rightarrow c\tau)$, which corresponds to $(x, y) = (0.6, 0.5)$. For the second one we do not want to pick extreme values of λ_R , as we could run into the regime of a “fat” leptoquark, namely having a width comparable to its mass. So we restrict ourselves to the best fit point $(0.16, 2.0)$ that already gives a negligible branching fraction into the third generation states. We thus use these working points to generate concrete benchmarks by picking two values for the leptoquark mass: $m_{S_1} = 500 \text{ GeV}$ and $m_{S_1} = 1000 \text{ GeV}$. We show the corresponding values of the couplings and branching ratios in Table 3, where we have assumed a negligible coupling of S_1 to the dark sector. We note that the solution of the $R_{D(*)}$ anomalies, being an off-shell interference with the SM amplitude, will not be affected by diluting the leptoquark visible decays,

¹As the neutrino flavor is not tagged, in principle the second index is not constrained. For simplicity we restrict it here to the third generation.

²Alternatively one could consider a right handed by explicitly introducing a right-handed neutrino that could serve as a dark matter candidate, see e.g [9].

³Defining $x = \lambda_L/m_{S_1}$ and $y = \lambda_R/m_{S_1}$ we have that the anomalies would scale with the product xy . Other constraints scale instead like x^2 or y^2 .

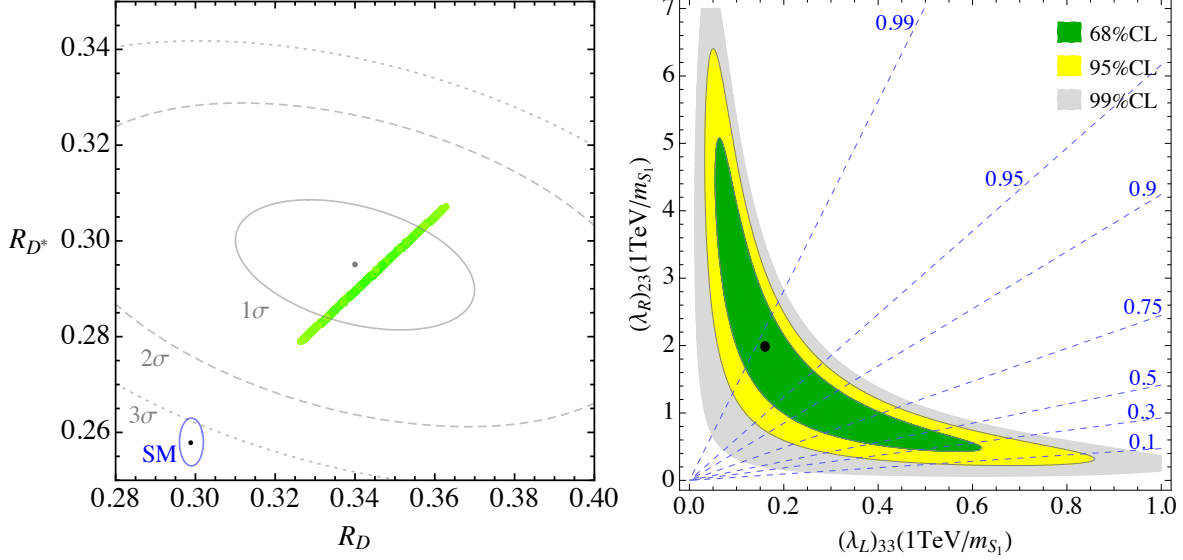


Fig. 1: Left: flavor fit to the charged current anomalies for $m_{S_1} = 1.5$ TeV (1σ region). The gray lines represent the present status in the measurements of the two observables, compared with the SM point (blue point and contour). Right: Viable parameter space from the fit of flavor and precision observables as function of λ/m_{S_1} . Blue dashed lines are iso-lines of the branching ratio $B(S_1 \rightarrow c_R \tau_R)$ assuming $y_\chi \ll (\lambda_L)_{33}, (\lambda_R)_{23}$ and $m_{S_1} \gg m_t$. The black dot represents the best-fit point.

m_{S_1} [GeV]	λ_L	λ_R	$BR(S_1 \rightarrow b\nu)$	$BR(S_1 \rightarrow t\tau)$	$BR(S_1 \rightarrow c\tau)$	$\Gamma(S_1)/m_{S_1}$
500	0.30	0.25	0.4049	0.3139	0.2812	4.42E-3
1000	0.6	0.5	0.3794	0.3571	0.2635	1.89E-2
500	0.08	1.0	0.0063	0.0049	0.9887	3.4E-2
1000	0.16	2.0	0.0063	0.0059	0.9877	8.06E-2

Table 3: Benchmark points compatible with the flavour anomalies. Here we have assumed negligible decays into the dark sector. Note the wide range of possibilities for the $c - \tau$ channel (from 25 % to roughly 100%) while the b and top decays have an upper bound of about 40 and 30 % respectively, and can actually become at the sub-percent level.

but it would rather loose the constraints coming from direct searches of S_1 , which we discuss in detail in Section 5..

Having established the parameter space in the λ_L, λ_R and m_{S_1} we will focus in the next section on the constraints given by dark matter observables: relic density, direct detection and indirect detection.

4. DARK MATTER CONSTRAINTS

In this section we study how the measured relic density and the null results of direct detection impact on our model. We start by noting that the direct detection rate is suppressed at 1-loop [JZ: draw box diagrams], however given the current σ_{SI} exclusions this suppression might not be enough to discard this observable. For the relic density we consider two distinct scenarios. On one hand we study the (co)-annihilation case, as done in [8], while on the other hand we also consider the conversion-driven freeze-out (CDFO) scenario [14], also known as co-scattering [15]. The main idea behind this mechanism is that the self-annihilation of the dark matter candidate is negligible: the dark matter abundance arises instead from conversion processes

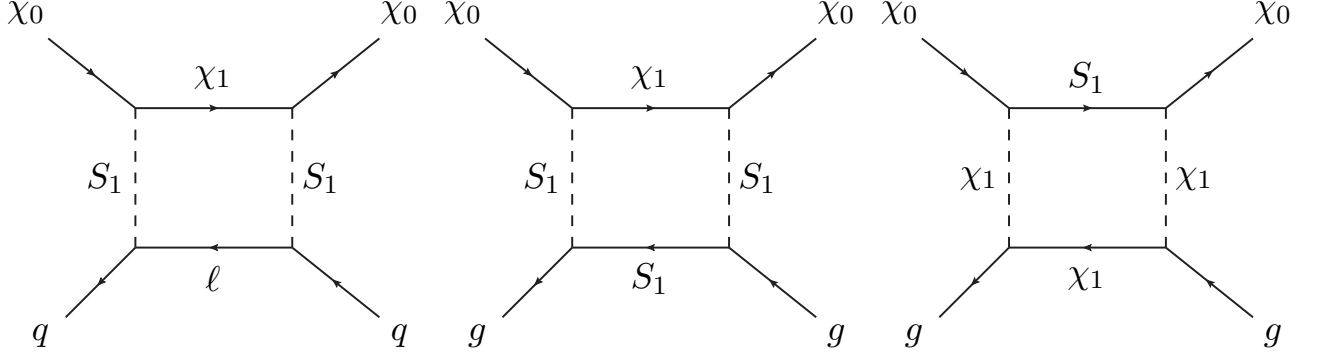


Fig. 2: Feynman diagrams for the direct detection of dark matter in our model at the lowest order in perturbation theory. **[JZ: Need to change some lines for second and third diagram. Please use your imagination].**

within the dark sector. Hence, this scenario requires small/tiny interactions between the SM and the DM candidate (y_{DM} in our case), thus rendering the $BR(S_1 \rightarrow \chi_1 \chi_0)$ negligible. This will thus affect the relevance of the collider signatures, that are discussed in detail in section 5.

4.1 Direct Detection

[JZ: Under study by GB, AG, DS, JB]

The scattering of χ_0 on a nucleon proceeds via 1-loop diagrams, which we show in figure 2. In the first diagram the loop include two leptoquark masses and the χ_1 mass, which are already heavy enough compared with the typical momentum transfer, so that would naively induce a mass suppression. In the second diagram one would have three leptoquark masses and a χ_1 mass, so that would be more suppressed than the diagram with three χ_1 and one S_1 in the loop. **[JZ: What follows is highly speculative and must be taken as such, the final answer will come from the explicit calculation of Andreas and Aoife.]** We can obtain a rough estimate of the size of these contributions by first integrating out the S_1 . We then would end with

- a 1-loop bubble with χ_1 and a lepton propagating in the loop and two effective couplings.
- a **[JZ: not sure about this one]** tree level diagram with $\chi_0 g \rightarrow \chi_0 g$ via a χ_1 exchange.
- a 1-loop triangle with χ_1 running in the loop and one effective $\chi_1 - \chi_1 - \chi_0 - \chi_0$ vertex.

Among the three possibilities, the third one is naively the less suppressed one since it has only one effective coupling less, and the lowest power in m_{S_1} .⁴ Hence the diagram scales as

$$\frac{1}{4\pi m_{S_1}} y_{DM}^2 \alpha_s * \frac{8\pi}{9\alpha_s} m_P f_{T,G} \sim \frac{0.2}{m_{S_1}} y_{DM}^2, \quad (2)$$

and thus the suppression is not very high: nowadays 1-loop EW corrections and 1-loop QCD corrections for WIMPS are relevant, and here we are at a similar level. **[JZ: Here I tried to conclude that we need the calculation, but once we have the final result we can use this digression as a “a posteriori” justification.]**
[JZ: end of speculation]

⁴Of course one can also integrate out χ_1 and directly write the $\chi_0 \bar{\chi}_0 G_{\mu\nu}^a G^{a\mu\nu}$, but then one would lose the explicit couplings and masses

4.2 Relic Density

[JZ: Coannihilation done with Micromegas. CDFO: Under study by GB, JH, AL, AG, JB]

Preliminary results using the LQ solution to the flavor anomalies and satisfying the correct relic density are displayed in Fig. 3.

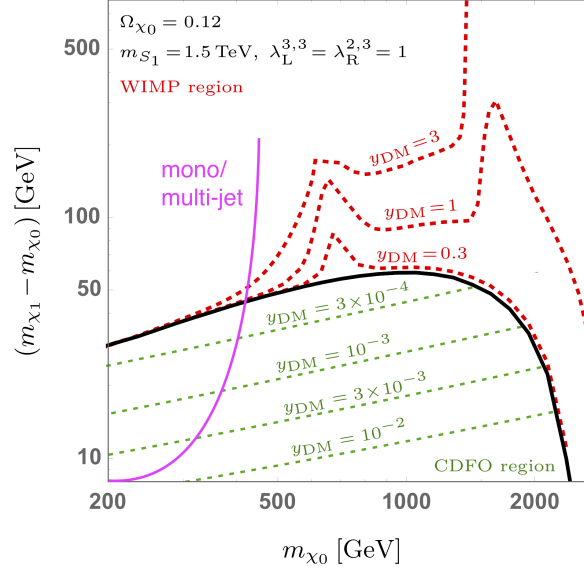


Fig. 3: Parameters space in the $m_{\chi_0} - \Delta = m_{\chi_1} - m_{\chi_0}$ plane satisfying $\Omega h^2 = 0.12$. The solid black line denotes the boundary between the coannihilation (CA) and the conversion-driven freeze-out (CDFO) regimes. The dashed lines also indicate the specific value of Y_{dm} . We also overlay a naive hand-waving estimate of the mono-jet reach (see Section 5.2).

4.3 Indirect Detection

[JZ: JH and AG want to write something about it.]

Indirect detection constitutes an important probe of the self-annihilating nature of dark matter. In the considered model annihilation today dominantly takes place either via the $2 \rightarrow 2$ process $\chi^0 \chi^0 \rightarrow S_1 S_1$, if $m_{S_1} < m_{\chi^0}$, or via $2 \rightarrow 4$ or loop-induced $2 \rightarrow 2$ processes otherwise. [Right?] Figure 6 shows an exemplary $2 \rightarrow 4$ annihilation diagram. As these processes are suppressed by the off-shell S_1 propagator (or loop-suppressed) we expect small annihilation rates. In particular, if annihilation during freeze-out proceeds dominantly via $\chi^0 \chi^\pm$ co-annihilation or pair-annihilation of χ^\pm , the relic density constraint does not require the dark matter self-annihilation rate to be large and hence we expect it to fall below the sensitivity of indirect detection experiments.

In Figure 5 we show an exemplary gamma-ray and antiproton spectra per annihilation for a benchmark point with $m_{\chi^0} = 150$ GeV, $m_{\chi^\pm} = 600$ GeV and $m_{S_1} = 1$ TeV. Note that as long as $m_{S_1} > m_{\chi^0}$ (and, of course, $m_{\chi^\pm} > m_{\chi^0}$) the masses m_{S_1} and m_{χ^\pm} are not expected to have a significant effect on the shape of the spectrum but mainly change the annihilation cross section, *i.e.* the total normalization of the signal. We also compare the spectra to the ones for annihilation into $b\bar{b}$ which is an often quoted reference channel in the literature (choosing the same dark matter mass). While the gamma-ray spectrum is very similar to the one for $b\bar{b}$, the antiproton spectrum is slightly more peaked. However, it does not exhibit a distinct feature

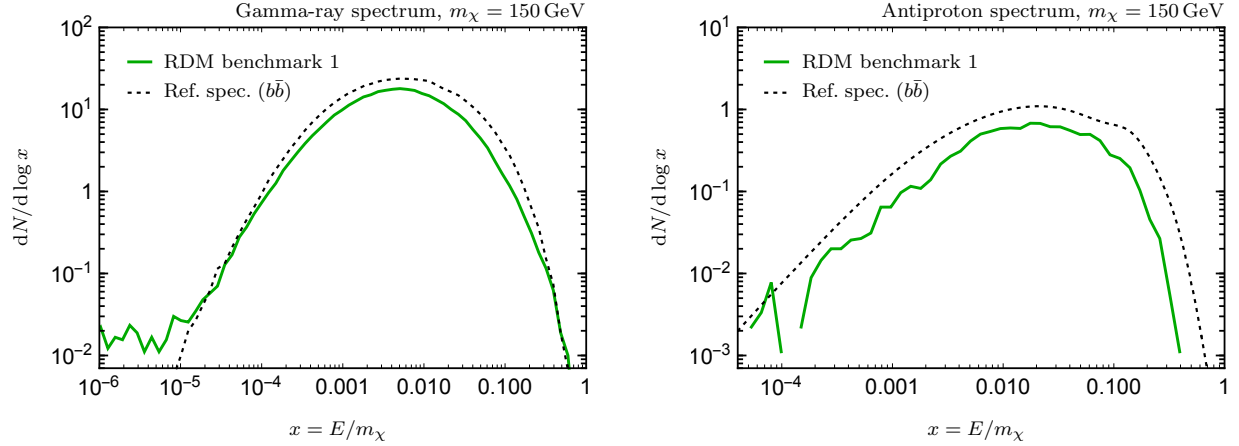


Fig. 4: Exemplary gamma-ray (left panel) and antiproton spectra (right panel) for dark matter annihilation of the benchmark point with $m_{\chi^0} = 150$ GeV, $m_{\chi^\pm} = 600$ GeV and $m_{S_1} = 1$ TeV (green curves). For comparison we show the corresponding reference spectra for annihilation into $b\bar{b}$ (black dotted curves).

that is expected to alter the constraints with respect to the case of $b\bar{b}$ drastically. Accordingly, we can use the limits on $b\bar{b}$ for an order-of-magnitude estimate of indirect detection limits in our model and use them to asses their relevance. *[Just as a proposal. Needs to be further checked, of course.]*

5. LHC CONSTRAINTS

Our model contains three new fields that are probed by several LHC searches, which generically fall into two categories. On one hand, we have direct searches for leptoquarks (S_1), both for single and double production. On the other hand we have the full spectrum of missing energy (MET) searches targeting dark matter observables, in our case driven by pair production of χ_1 via gauge interactions. As a hybrid of both categories, the CMS search for leptoquark plus dark matter [16], inspired by the Coannihilation Codex [8], gives not only interesting constraints on the parameter space, but moreover it would allow to establish the connection between flavor anomalies and dark matter, in a post-discovery scenario.

In each of the categories described above, we will consider both a) existing searches and b) novel searches (for instance, the aforementioned LQ + MET search of Ref [16] only applies if the leptoquark decays to muons, but it is not applicable for e.g: electron decays).

We note that the actual mechanism underlying the production of the dark matter abundance has phenomenological implications. Two distinct scenarios arise, depending on the size of y_{DM} versus $\lambda_{L,R}$. For y_{DM} comparable to the S_1 couplings to leptons and quarks all S_1 decay modes $b\nu, c\tau, t\tau, \chi_1\chi_0$ have comparable branching fractions, as shown in Figure 7. In this scenario all three kind of searches (LQ, MET, LQ + MET) are relevant and can be used to constraint the model or, in the case of a signal, would allow to establish this model and measure its parameters. Also shown in Figure 7 are the cross-sections for pair production of χ_1 and single and pair production of S_1 . As can be seen, the χ_1 production is dominant, unless $m_{S_1} \ll m_{\chi_1}$. The χ_1 channel, however, can be challenging to detect if χ_1 and χ_0 are nearly degenerate. Hence both LQ and MET searches can be relevant for constraining or detecting the model.

In the case of CDFO, we have seen from Figure 3 that $y_{DM} \lesssim 10^{-2}$ and hence we would have only the signatures in LQ searches and in MET searches. However, if in the $\chi_1 \rightarrow \chi_0 l q$ decay one could resolve the final state lepton and quarks, one would have an additional handle to establish a link between the

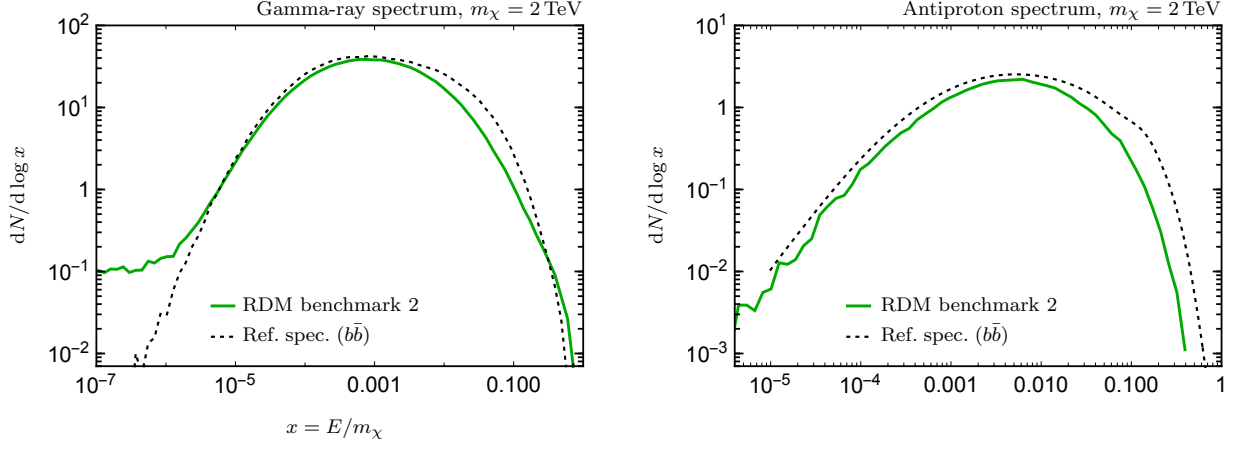


Fig. 5: Exemplary gamma-ray (left panel) and antiproton spectra (right panel) for dark matter annihilation of the benchmark point with $m_{\chi^0} = 2$ TeV, $m_{\chi^\pm} = 2.5$ TeV and $m_{S_1} = 1.5$ TeV (green curves). For comparison we show the corresponding reference spectra for annihilation into $b\bar{b}$ (black dotted curves).

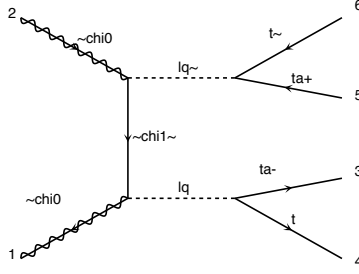


Fig. 6: Exemplary $2 \rightarrow 4$ dark matter annihilation diagram.

apparently uncorrelated signals in LQ and MET searches.

5.1 Leptoquark searches

[JZ: Under study by JB, GP, PP, JZ, AJ]

5.11 LQ pair searches

Pair production of LQs at the LHC proceeds via gauge couplings, as shown in the left panel of Fig 8.

Searches for visible decays of LQ pairs at ATLAS [17, 18, 19] and CMS [20, 21, 22], focus on both leptoquarks decaying in the same final state. In Ref. [19] five different searches are described. The first one is a search for LQ decaying into the $b\tau b\tau$ final state, based on an existing di-Higgs search in the same final state [23], albeit with different kinematics. The other four searches are reinterpretations of existing studies of supersymmetric particles: searches for stop pair production in the zero-lepton [24] and one-lepton channel [25] ($t\bar{t} + \text{MET}$), stop decays into staus [26] and a sbottom search [27] ($b\bar{b} + \text{MET}$). Among these searches, what is relevant for our model are the final states of $b\tau b\tau$, which correspond to the decay of both leptoquarks in the $t\tau$ final state, and the search for $b\bar{b} + \text{MET}$ which covers the case where both leptoquarks

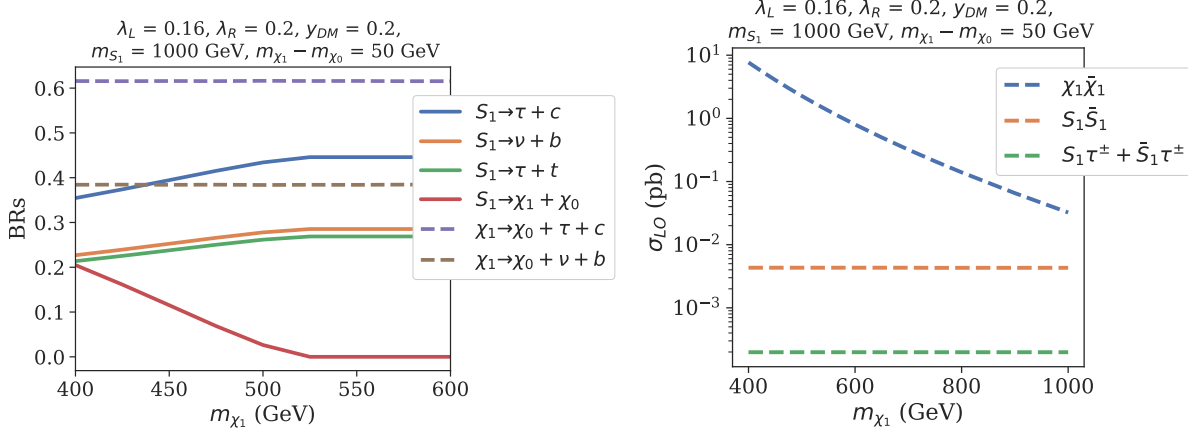


Fig. 7: Branching ratios (left) and production cross-sections at the 13 TeV LHC (right) for S_1 and χ_1 as a function of the χ_1 mass. The mass difference between χ_1 and χ_0 is kept as 50 GeV, $y_\chi = 0.2$ and the other parameters are: $\lambda_L = 0.16$, $\lambda_R = 0.2$ and $m_{S_1} = 1$ TeV.

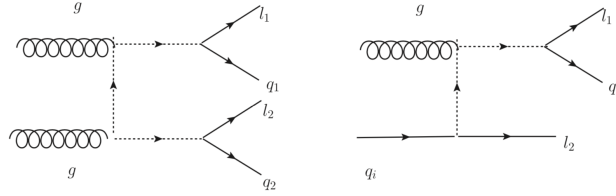


Fig. 8: Leptoquark production at the LHC: single (left) and double (right), considering visible decays.

decay into $b\nu$. For any choice of the coupling, and barring effects from the top mass, we would have that $BR(S_1 \rightarrow t\tau) \approx BR(S_1 \rightarrow b\nu)$, in contrast to the ATLAS study where $BR(S_1 b\nu) = 1 - BR(S_1 \rightarrow t\tau)$ is assumed. Thus, in order to achieve an optimal coverage of the parameter space, one should also include the final state $b\nu t\tau$, which we dubbed the “mixed” visible leptoquark search. We present in Fig 9 the corresponding branching ratios into $t\tau$ (solid red) and $b\nu$ (solid blue) for the scenario where only λ_L is turned on, together with the reach in the $t\tau t\tau$ (dashed red), $b\nu b\nu$ (dashed blue) and our proposed search $t\tau b\nu$ (dashed green).

We thus see that above 500 GeV the mixed search has the best coverage, and thus we will adopt this search to carry out our projections for the HL-LHC⁵. In view of these results we encourage the experimental collaborations to design a full-fledged analysis targeting the mixed decay. However it is clear from the fits to the charged-current flavor anomalies of Figure ?? and from our benchmark points shown in Table 3 that the search based exclusively on the third generation final states is insufficient to cover the $R_{D^{(*)}}$ -compatible parameter: since λ_R is always larger than λ_L , S_1 decays predominantly into the $c\tau$ final state. Thus a search including this final state (in particular the $c\tau c\tau$ channel) would be needed. In view of the impressive results achieved in final states with two c -tagged quarks [] [JZ: Need citations from Giacomo], this analysis

⁵[JZ: This last sentence is from Giacomo. I am not sure if for the proceedings we will do HL-LHC, but I agree with the philosophy of using only the best search for LQ pairs.]

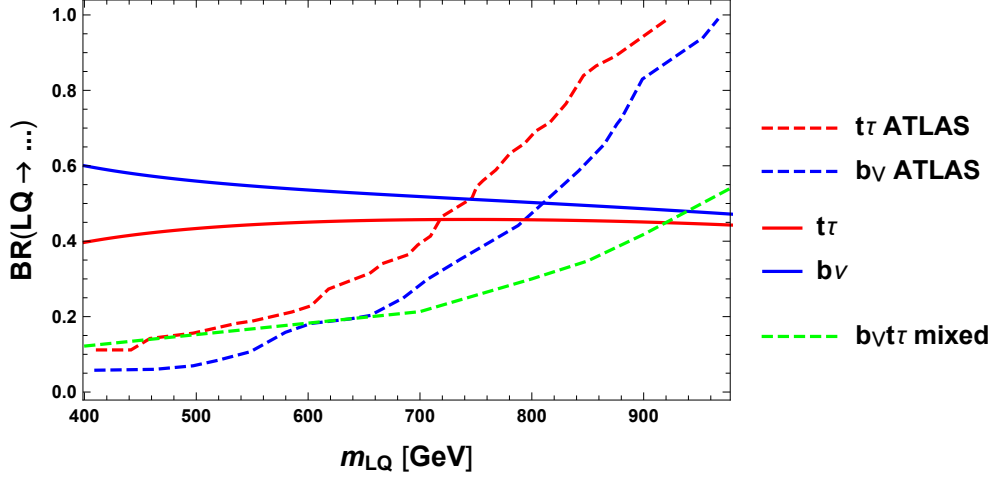


Fig. 9: Coverage of the different LQ pair searches with decays into third generation fermions. We show in solid lines the branching ratio for the case where only λ_L is non-zero, namely where the leptoquark decays exclusively into $b\nu$ (blue) and $t\tau$ (red). Note that both branching fractions should be equal if the top mass were negligible with respect to m_{S_1} . We also present in dashed lines the reach of the ATLAS search for $t\tau t\tau$ (red), $b\nu b\nu$ (blue), taken from [19], as well as our proposed search in the $t\tau b\nu$ channel (green). The latter final state provides the best coverage of the parameter space provided that $m_{S_1} \gtrsim 500$ GeV. *l*

should be feasible, however is outside the scope of this proceeding. **[JZ: Does it mean that we want to do it for the paper?]**

5.12 LQ associated production (with lepton and/or jet)

[JZ: In charge: JZ, AB, DS, AJ]

A single leptoquark can also be produced in association with a SM fermion, as shown in the right panel of Fig 8. For our particular choice of couplings, we expect that one can have some sensitivity if this fermion is a charged lepton, hence if $l_2 = e, \mu, \tau$.

[JZ: To the best of my understanding this is under study by David, Giacomo and others. At the current stage I would be happy to point out to their study within the same proceedings.]

5.2 Dark matter (missing energy) searches

Since the χ_1 particle is the lightest new particle with non-trivial SM quantum numbers, its production is strongly constrained by LHC searches, and it can only be “hidden” if χ_1 and χ_0 are close in mass. The LHC production is depicted in Fig. 10. The usual strategy against a compressed spectra is to boost the system with additional radiation, leading to the mono-X (typically jet) signals.

However, if the SM decay products in the $\chi_1 \rightarrow \chi_0$ are soft enough to be reconstructed (but probably not to triggered on) the LHC sensitivity gets greatly enhanced, as shown in e.g: [28] for MSSM electroweakinos and soft-leptons. However, the mass gap can be small enough such that the soft decay products fail to pass the reconstruction thresholds, in which case the pair production of χ particles can only be constrained by mono-jet searches. We stress that this is an unavoidable bound, that, for a given Δ , sets a lower mass on the dark sector masses. We will thus ignore here the MET searches that also include resolved (soft or hard) leptons. **[JZ: This last sentence needs to be revisited depending on what is available in**

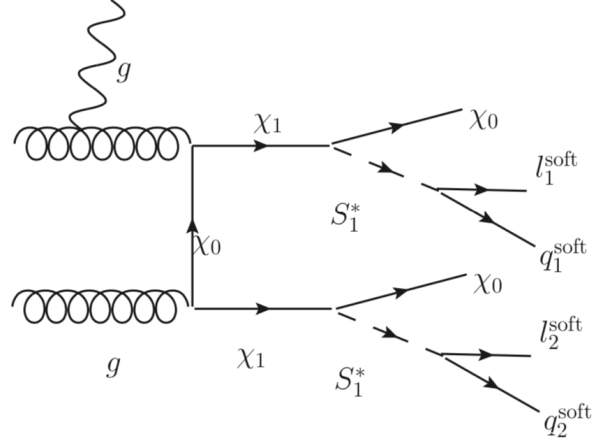


Fig. 10: Monojet (plus soft leptons and quarks) signatures.

MadAnalysis, CheckMATE or similar].

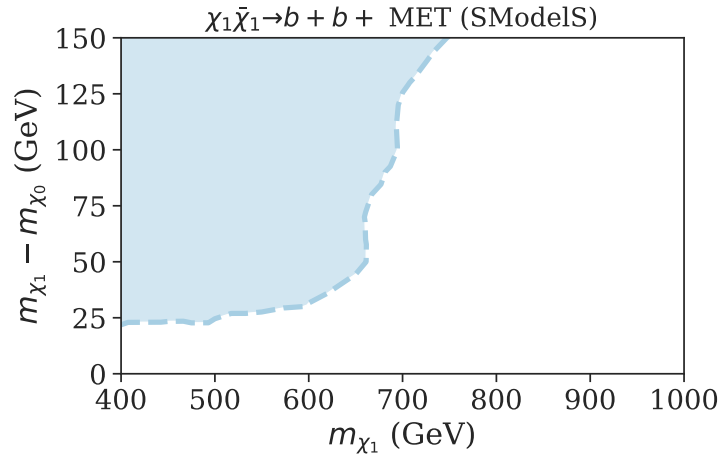


Fig. 11: Region in the $m_{\chi_1} - m_{\chi_0}$ vs m_{χ_1} plane excluded by LHC MET searches. The remaining model parameters are $y_\chi = 0.2$, $\lambda_L = 0.16$, $\lambda_R = 0.2$ and $m_{S_1} = 1$ TeV. The shaded region corresponds to the parameter space excluded by ATLAS and CMS searches for final states containing one or more b-jets and missing energy. *The signal efficiencies are assumed to be the same as for sbottom pair production followed by $\tilde{b} \rightarrow b + \chi_1^0$ decays. We do not take into account possible effects due to the 3-body decay of χ_1 ($\chi_1 \rightarrow b + \chi_0 + \nu$).*

5.3 Resonant lepto-quark + MET search

[JZ: Benj wants to recast the CMS study, [16]. AJ will help him.].

6. CONCLUSIONS

The charged-current flavor anomalies hint at the presence of leptoquarks near or at the TeV scale. Here we have studied the connection between these models and dark matter, which necessarily requires to add new

particles and couplings. Employing a simplified model with only 6 parameters we have scanned the parameter space vis-a-vis the aforementioned flavor anomalies, relic density, direct detection and LHC constraints.

We have seen that when taken all these constraints simultaneously one is left with two possible scenarios: either the dark sector couples to the leptoquark mediator with a similar strength than the one required from taking the $R_{D^{(*)}}$ anomaly at face-value, which then implies a traditional freeze-out scenario to account for the current abundance of dark matter, or the leptoquark couples faintly to the dark sector, which in turn implies that the dark matter abundance arises from the conversion-driven freeze-out (co-scattering) mechanism. In the second scenario the leptoquark branching fraction into the dark sector is negligible, and thus the phenomenology will consist of seemingly disconnected leptoquark “anomaly-inspired” and traditional missing energy + X signatures. In the latter case, depending on the “compression” between the dark sector particles, one can resolve the leptons and quarks from the $S_1 \rightarrow \chi_1 \chi_0 \rightarrow lq \chi_0 \chi_0$ decay chain, which would then allow to establish a firm connection between both new physics signals. In the case where the branching fraction into the dark sector is non-negligible, then the strongest indication of the leptoquark-dark matter connection is through the pair production of leptoquarks with one decaying into the dark sector and another one into hard leptons and quarks. Since this search is only being conducted currently by the CMS collaboration, we urge ATLAS to undertake this key study for a comprehensive dark matter program going beyond the mere annihilation into singlet final states.

Along this work we have pointed out the existence of two important holes in the campaign to optimally cover the leptoquark parameter space. On one side we have noted that for leptoquarks decaying into the third generation fermions (almost) exclusively, a search in the $b\nu t\tau$ should be added to the existing ones looking into $b\nu b\nu$ and $t\tau t\tau$, where one can benefit from a larger branching fraction, and devise cuts to keep the background under control, which we have demonstrated with a simple analysis. On the other side, noting that the solutions to the $R_{D^{(*)}}$ anomalies involve larger couplings connecting second generation quarks with third generation leptons, we advocate to study the $c\tau c\tau$ final state, and if possible and depending on the c -tagging efficiencies, also include the mixed cases, e.g. $c\tau t\tau$ or $b\nu c\tau$ final states.

Our results show that... **[JZ: describe final parameter space allowed]**. Naively rescaling our results for the HL-LHC we find that (**[JZ: hopefully]**) the parameter space favored by the flavor anomalies will be fully covered with just 1000 fb^{-1} of data. **[JZ: Maybe we will leave the projections for the paper?]**

ACKNOWLEDGEMENTS

We would like to thank AAA and BBB for useful discussions. The work of XXX was supported (in part) by

A Appendix A

References

- [1] R. Aaij *et al.*, **LHCb** Collaboration *JHEP* **08** (2017) 055, [1705.05802].
- [2] R. Aaij *et al.*, **LHCb** Collaboration *Phys. Rev. Lett.* **122** (2019), no. 19 191801, [1903.09252].
- [3] R. Aaij *et al.*, **LHCb** Collaboration *Phys. Rev. Lett.* **115** (2015), no. 11 111803, [1506.08614].
[Erratum: *Phys. Rev. Lett.* 115, no. 15, 159901 (2015)].
- [4] R. Aaij *et al.*, **LHCb** Collaboration *Phys. Rev. Lett.* **120** (2018), no. 17 171802, [1708.08856].
- [5] R. Aaij *et al.*, **LHCb** Collaboration *Phys. Rev.* **D97** (2018), no. 7 072013, [1711.02505].

- [6] M. Blanke, in *29th International Conference on Lepton and Photon Interactions (LP2019) Toronto, Ontario, Canada, August 5-10, 2019*, 2019. 1908.09713.
- [7] F. S. Queiroz, K. Sinha, and A. Strumia, *Phys. Rev.* **D91** (2015), no. 3 035006, [1409.6301].
- [8] M. J. Baker *et. al.*, *JHEP* **12** (2015) 120, [1510.03434].
- [9] A. Azatov, D. Barducci, D. Ghosh, D. Marzocca, and L. Ubaldi, *JHEP* **10** (2018) 092, [1807.10745].
- [10] A. Crivellin, D. Müller, and T. Ota, *JHEP* **09** (2017) 040, [1703.09226].
- [11] D. Buttazzo, A. Greljo, G. Isidori, and D. Marzocca, *JHEP* **11** (2017) 044, [1706.07808].
- [12] D. Marzocca, *JHEP* **07** (2018) 121, [1803.10972].
- [13] A. Crivellin, D. Müller, and F. Saturnino, 1912.04224.
- [14] M. Garny, J. Heisig, B. Lülfi, and S. Vogl, *Phys. Rev.* **D96** (2017), no. 10 103521, [1705.09292].
- [15] R. T. D’Agnolo, D. Pappadopulo, and J. T. Ruderman, *Phys. Rev. Lett.* **119** (2017), no. 6 061102, [1705.08450].
- [16] A. M. Sirunyan *et. al.*, *CMS Collaboration Phys. Lett.* **B795** (2019) 76–99, [1811.10151].
- [17] G. Aad *et. al.*, *ATLAS Collaboration Eur. Phys. J.* **C76** (2016), no. 1 5, [1508.04735].
- [18] M. Aaboud *et. al.*, *ATLAS Collaboration Eur. Phys. J.* **C79** (2019), no. 9 733, [1902.00377].
- [19] M. Aaboud *et. al.*, *ATLAS Collaboration JHEP* **06** (2019) 144, [1902.08103].
- [20] A. M. Sirunyan *et. al.*, *CMS Collaboration Eur. Phys. J.* **C78** (2018) 707, [1803.02864].
- [21] A. M. Sirunyan *et. al.*, *CMS Collaboration Phys. Rev.* **D98** (2018), no. 3 032005, [1805.10228].
- [22] A. M. Sirunyan *et. al.*, *CMS Collaboration JHEP* **03** (2019) 170, [1811.00806].
- [23] M. Aaboud *et. al.*, *ATLAS Collaboration Phys. Rev. Lett.* **121** (2018), no. 19 191801, [1808.00336]. [Erratum: *Phys. Rev. Lett.* 122, no. 8, 089901 (2019)].
- [24] M. Aaboud *et. al.*, *ATLAS Collaboration JHEP* **12** (2017) 085, [1709.04183].
- [25] M. Aaboud *et. al.*, *ATLAS Collaboration JHEP* **06** (2018) 108, [1711.11520].
- [26] M. Aaboud *et. al.*, *ATLAS Collaboration Phys. Rev.* **D98** (2018), no. 3 032008, [1803.10178].
- [27] M. Aaboud *et. al.*, *ATLAS Collaboration JHEP* **11** (2017) 195, [1708.09266].
- [28] P. Schwaller and J. Zurita, *JHEP* **03** (2014) 060, [1312.7350].